HTML ABSTRACT + LINKS

JOURNAL OF APPLIED PHYSICS VOLUME 95, NUMBER 9 1 MAY 2004

In situ second-harmonic generation measurements of the stability of Si(111)–H and kinetics of oxide regrowth in ambient

D. Bodlaki and E. Borguet[a)]
Department of Chemistry and Surface Science Center, University of Pittsburgh, Pittsburgh, Pennsylvania 15260

(Received 10 October 2003; accepted 13 January 2004)

The oxidation of H terminated silicon surfaces is a significant and controversial problem in silicon device fabrication. Second-harmonic generation rotational anisotropy (SHG–RA) provides a convenient means to monitor the chemical state of the Si surfaces, and to follow the conversion of H terminated surface to SiO_2 by oxidation as a function of time in ambient. The change in SHG–RA of Si(111)–H was shown to correlate well with the ellipsometric thickness. SHG is sensitive to the initial stage of oxidation (induction period) as well as to the logarithmic oxide growth. SHG is sensitive to the electronic properties of the surface, therefore it is a sensitive probe of the quality of H terminated Si(111) surface. Under ambient conditions, (20% relative humidity, 23 °C) the initial oxidation rate is at most 2×10^{-6} ML/s. © *2004 American Institute of Physics.*
[DOI: 10.1063/1.1664024]

I. INTRODUCTION

The passivation of semiconductor interfaces and the stability of passivated interfaces under reactive conditions is a topic of interest to physical scientists and technologists alike.[1,2] Remarkably, it has been shown that atomically flat passivated Si(111) surfaces can be generated by simple wet chemical techniques.[3] NH_4F solutions can terminate the Si dangling bonds by H atoms to form monohydride Si species on Si(111).[3] This passivated surface is the starting point for a number of processes that transform the chemical and physical nature of the semiconductor interface.[4] The stability of H passivated Si surfaces with respect to oxidation is critical to the subsequent processing steps. Oxidation of H terminated Si results in the regrowth of the native oxide. This is an impediment to subsequent chemical modification such as alkylation, for example. The regrowth of native oxide is to be avoided as it has been shown to degrade the low temperature growth of high quality epitaxial Si films.[5] The presence of native oxide also impacts the quality and precise thickness of thin gate oxides grown on initially passivated surfaces.[6]

While an important objective is the determination of the stability of passivated surfaces, there has been some controversy over the measured growth rates of native oxide on H terminated Si surfaces in ambient, resulting in an on-going debate over the time needed for an oxide monolayer to form on the low index surfaces of silicon passivated by hydrogen termination.[7–9] Estimates range from 1 hour to several weeks.[5,7,8,10–12] The differences are in part related to the storage conditions (relative humidity, exposure to light), wet-chemical treatments (metal contamination, water rinse, oxygen dissolved in chemicals) and properties of the sample [surface orientation, doping, . . .].

Using x-ray photoelectron spectroscopy (XPS) to probe surface oxygen, an induction period of 5 days for NH_4F treated Si(100) and 1 week for HF treated Si(100) was reported.[7,8] The induction time was characterized by very slow oxidation, after which oxidation accelerated in a logarithmic fashion.[7,8] Formation of a monolayer equivalent of chemisorbed oxygen, (one O atom per surface Si atom) took a week (approximately 10^4 min).[7] Previous studies had reported logarithmic oxide growth without an induction period.[11,12] Another study found that the oxide growth of HF treated Si(111) stored in ambient is best described by a $(t)^{1/2}$ law with a 10 min "incubation time."[13] Clearly, there is a controversy about the duration of the slow, induction phase of oxidation.

High-resolution electron energy-loss spectra (HREELS) studies suggest that the initial oxidation on Si(100) occurs via O incorporation in a nonstoichiometric (SiO_x) matrix, i.e., O inserts in Si backbonds forming a Si–O–Si network.[7,9] HREELS data indicates substantial Si–H remaining on the Si(100) surface after a week, though most of it is associated with oxygen backbonded Si.[7,9,10] In fact, formation of $HSiO_nSi_{3-n}$ ($n=1,2,3$) moieties, i.e., one Si atom with one H ligand and n O ligands, was observed by Fourier-transform infrared.[5] The observation of an intact Si–H bond is consistent with the high contact angles measured for NH_4F treated Si(100) over a period of weeks.[8]

Assuming that the O is inserted between the first and the second layers of silicon atoms, a maximum O coverage of 3 ML can be reached before SiO_2 species (not suboxide) oxide formation proceeds. The formation of a SiO_2 monolayer on Si(100), equivalent to a 3-Å-thick oxide layer, requires 15–20 days of storage in air.[7] XPS results indicate that the SiO_2 peak does not appear for almost 2 weeks, though SiO_x appears after a few days.[8] Oxide growth is accompanied by oxide charge development evaluated at 10^{11} charges/cm^2.[7] The presence of this oxide charge leads to band bending.[7]

[a)]Author to whom correspondence should be addressed; electronic mail: borguet@pitt.edu

 © 2004 American Institute of Physics

Downloaded 06 Sep 2009 to 129.32.36.173. Redistribution subject to AIP license or copyright; see http://jap.aip.org/jap/copyright.jsp

The present work investigates the oxidation of Si(111)–H surface by second-harmonic generation rotational anisotropy (SHG–RA) at 800 nm. The changes in the rotational anisotropy upon oxidation of Si(111)–H further enhance our understanding of the origin of the SHG response at 800 nm. A number of techniques were used in parallel to SHG including ellipsometry, atomic force microscopy to determine the quality of the Si(111)–H surface and to follow the oxidation. We show that 800 nm SHG is sensitive to the electronic properties of the interface and can be used to probe the evolution of the chemical state of the Si interface. We found the initial oxidation rate to be 2×10^{-6} ML/s.

II. EXPERIMENT

n-type Si(111) wafers (*P* doped with ~30 Ω cm resistivity, $N_D\sim4\times10^{14}$ cm^{-3}, Motorola Phoenix, ~300 μm thick) were used in our experiments. H termination involved the following steps: cleaning in piranha solution {4:1 conc. H_2SO_4 [Fisher, trace metal grade]: 30% H_2O_2 [J.T. Baker, complementary metal–oxide–semiconductor (CMOS) grade]} for 10 min at 100 °C, followed by an SC2 clean, [1:1:4 30% H_2O_2: conc. HCl (J.T. Baker, CMOS grade): H_2O] for 10 min at 80 °C, and finally a second 10 min in piranha solution at 100 °C. At the end of the sequence the samples were thoroughly rinsed in ultrapure water (>18 MΩ cm).[14] This cleaning procedure will be termed as "piranha" cleaning in this article. For H termination the samples were immersed after "piranha" cleaning in 40% NH_4F solution (Transene, semiconductor grade) for 15 min to remove the oxide and H terminate the surface Si.[15] After immersion in NH_4F the samples were hydrophobic. Native oxide samples that were used as received were only subjected to a degreasing in trichloroethylene, acetone, and methanol for 10 min each at room temperature prior to experiments.

The ellipsometric thickness of the surface layer was measured on an ellipsometer (Gaertner Scientific, model L117) at a 70° angle of incidence and $\lambda=632.8$ nm. The typical ellipsometric thickness of the native oxide samples was 2.0 ± 0.05 nm. For H terminated Si(111), measured within 5 min of final NH_4F etch, a thickness of 0.17 ±0.05 nm was determined. We used $n\pm3.882$, $k=0.019$ for Si and $n=1.455$ for SiO_2 at 632.8 nm for calculating layer thickness where n is the real and k is the imaginary part of the complex refractive index.[16]

SHG–RA measurements were carried out to control the exactness of the crystal cut and the effects of wet chemical treatment.[17] In these experiments, the azimuthal angle, ϕ, was measured with respect to the $[2\bar{1}\bar{1}]$ direction. SHG measurements were carried out with 4 ps pulses from a Ti:sapphire regenerative amplifier operating at 1 kHz.[18] The *p*-polarized 800 nm beam was incident on the sample at 45° with respect to the surface normal. The fluence was typically 0.01 J/cm^2 generating an excited carrier density of 4 $\times10^{19}$ cm^{-3} near the surface.[19] The beam was optically filtered (Kopp Glass No. 2-63) to remove second harmonic photons (400 nm) and lightly focused to a beam diameter, determined using a knife edge technique, of 1.1 ± 0.1 mm.

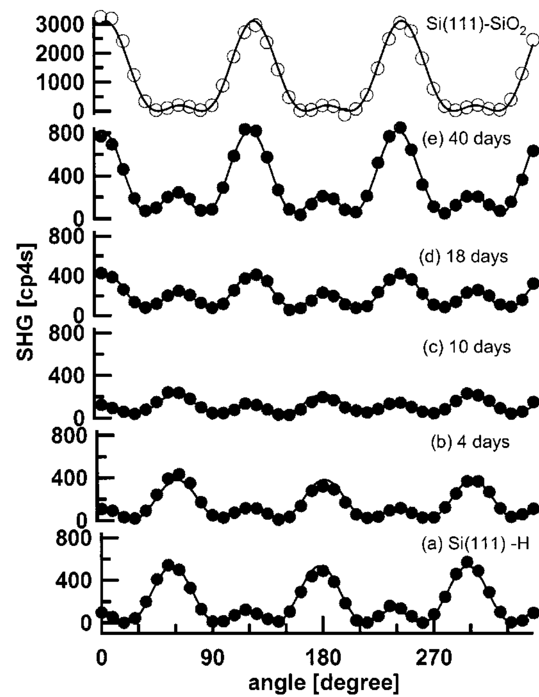

FIG. 1. Oxidation of Si(111)–H. The SHG rotational anisotropy pattern of H terminated (●) surfaces after (a) 10 min, (b) 4, (c) 10, (d) 18, and (e) 40 days of exposure to laboratory ambient (RH=20%). The sample was probed by SHG–RA on average every 3 days. The SHG–RA of an oxide covered Si(111) surface (○) is also shown (note scale difference).

The beam area was corrected for elliptical shape obtained at non-normal incidence. The reflected beam was sent to a monochromator (Acton Research, 300i, 2400 groove/mm grating) after short pass filtering (Kopp Glass No. 4–94) to block 800 nm photons. A liquid nitrogen cooled charge coupled device camera (Princeton Instrument, CCD30-11) was used in single element detection mode. An analyzing polarizer was set to pass *p*-polarized SH photons. The quadratic nature of second-harmonic response was verified in the power range explored.[20] The SHG response was normalized to the SHG signal from the native oxide sample at the azimuth of maximum SHG ($\phi=0°$).

Care was taken in choosing the experimental conditions: photo-oxidation was minimized by placing the incident beam at least 2 mm away from the axis of rotation.[21] Thus each data point in the SHG–RA experiment received less than 20 s of illumination, resulting in negligible photoreaction (0.005 ML of oxide formation) as a consequence of the SHG measurement.

III. RESULTS AND DISCUSSION

A. Rotational anisotropy of Si(111)–SiO$_2$ and Si(111)–H

H terminated and oxide covered Si(111) surfaces can be distinguished by their distinct SHG–RA patterns (Fig. 1). The overall magnitude of the SHG–RA of H–Si(111) is much smaller than for oxide covered Si(111) surfaces. The SHG–RA pattern can be analyzed with the following phenomenological formula:

$$I_{pp}(2\omega)\propto|A_{pp}+B_{pp}\cos(3\phi)|^2, \tag{1}$$

Downloaded 06 Sep 2009 to 129.32.36.173. Redistribution subject to AIP license or copyright; see http://jap.aip.org/jap/copyright.jsp

TABLE I. Magnitude of isotropic (A_{pp}) and anisotropic (B_{pp}) components and their relative phase, Δ_{AB} for Si(111)-native oxide and H terminated surfaces at 800 nm.

	A_{pp}	B_{pp}	B_{pp}/A_{pp}	Δ_{AB}	$[[(B_{pp}/A_{pp})-\cos\Delta]^2]$
Si(111)-oxide	22.6	36.2	1.6	12	0.4
Si(111)–H	6.3	16.6	2.6	162	12.6

TABLE II. Nonlinear susceptibilities for Si(111)–SiO_2 and Si(111)–H interface at 800 nm. Phases of complex nonlinear susceptibilities relative to bulk ξ term are indicated in parenthesis. Notation for the nonlinear susceptibility components is the same as in Ref. 25.

	∂_{11}/ξ	$(\gamma/\varepsilon_2+\partial_{31})/\xi$	∂_{15}/ξ	$\partial_{33}-\partial_{31}/\xi$
Si(111)–SiO_2	0.167 (180)	0.014 (−157)	0.217 (157)	0.768 (23)
Si(111)–H	0.113 (180)	0.0042 (−146)	0.103 (155)	0.26 (131)

where A_{pp} and B_{pp} are the isotropic and anisotropic contributions to the nonlinear susceptibility, respectively.[22] A_{pp} and B_{pp} parameters are complex numbers, whose relative phase Δ_{AB} can be defined via

$$\frac{B_{pp}}{A_{pp}}=\frac{|B_{pp}|}{|A_{pp}|}\exp(-i\Delta_{AB}). \tag{2}$$

The SHG–RA pattern is the result of interference between the complex A_{pp} and B_{pp} terms. The reversal in the sequence of large peaks and small peaks in the RA patterns for the two systems is primarily a consequence of the different relative phase between A_{pp} and B_{pp} for H–Si(111) and SiO_2/Si(111). The fits to Eq. (1) are shown in Fig. 1, and the magnitude of the A_{pp} and B_{pp} parameters as well as their relative phase (Δ_{AB}) for SiO_2/Si(111) and H–Si(111) are reported in Table I.

To understand the microscopic origin of the difference in the phase Δ_{AB} of the Si(111)–SiO_2 and Si(111)–H, we have extracted the microscopic nonlinear susceptibilities from the values of the complex A_{pp} and B_{pp} at 800 nm. The coefficients A_{pp} and B_{pp} can be expressed in terms of the surface and bulk nonlinear susceptibilities as follows:

$$A_{pp}=A_p\left\{a_{1pp}\xi+a_{2pp}\left[\frac{\gamma}{\varepsilon(2\omega)}+\partial_{31}\right]+a_{3pp}(\partial_{31}-\partial_{33})+a_{4pp}\partial_{15}\right\}, \tag{3}$$

$$B_{pp}=A_p(b_{1pp}\xi+b_{2pp}\partial_{11}). \tag{4}$$

The nonlinear susceptibility elements ∂_{11}, ∂_{15}, ∂_{31}, ∂_{33} describe the electric-dipole response of the surface.[23,24] The nonlinear susceptibility ∂_{11} contributes to the anistropic part (B_{pp}) of the SHG signal. The elements ∂_{15}, ∂_{31}, ∂_{33} describe the isotropic part (A_{pp}) of the SHG signal. The total nonlinear response has isotropic and anisotropic electric-quadrupole contributions from the bulk, described by the bulk nonlinear susceptibilities γ and ξ, respectively. The a and b coefficients as well as A_p in Eqs. (3)–(4), depend only on the linear dielectric parameters of the interface and the angle of incidence.[24] Following the analysis described in the literature, we extracted the relative magnitude and phase of the surface nonlinear susceptibilities with respect to the bulk susceptibility (Table II).[24,25]

The magnitude of all the nonlinear susceptibility components decreases going from oxide to H termination, in accordance with the decrease in the overall decrease in the SHG intensity (Table II). The phase of the ∂_{11}, $(\gamma/\varepsilon_2+\partial_{31})$, ∂_{15} components changes only slightly, but the phase of the $(\partial_{33}-\partial_{31})$ component changes dramatically, from 23° for Si(111)–SiO_2 to 131° for Si(111)–H (Table II). The ∂_{33} component governs the nonlinear polarization component perpendicular to the surface and is induced by the fundamental electric fields perpendicular to the surface. Mitchell *et al.* observed the same trends of the nonlinear susceptibilities of the Si(111)–H and Si(111)–SiO_2 interfaces at 775 and 830 nm as described earlier.[25]

A correlation between the chemical shifts in the Si 2p core level photoelectron spectra of the modified surfaces and the A_{pp} and B_{pp} parameters was found for the decyl,–H, –Cl, and –oxide terminated Si(111).[25] A linear relationship exists between the shift of the core-level binding energies and the electronegativity difference between the adsorbate ("C," H, Cl, and O) and the substrate (Si).[26] The electronegativity difference provides a measure of the polarity of a bond between the adsorbate and the substrate atom. Polarization of the surface bonds should increase the SHG response. The electronegativity of oxygen is greater than that of hydrogen (3.44 for O, 2.2 for H, 1.9 for Si). The Si–O bond is more polar than the Si–H bond. This difference in the bond polarity can explain the decrease in the magnitude of the nonlinear susceptibilities components ∂_{11}, $(\gamma/\varepsilon_2+\partial_{31})$, ∂_{15}, $(\partial_{33}-\partial_{31})$ and the increase in the phase of $(\partial_{33}-\partial_{31})$ as we go from Si(111)–SiO_2 to Si(111)–H.[27] Bond polarity differences are also successful in explaining the changes in SHG upon chemical modification of germanium interfaces.[24,28]

The dramatic change in the ∂_{33} component points to possibility of an electric field induced SH (EFISH) contribution. The SiO_2 accommodates charges which in turn create an electric field at the Si(111) interface.[29] On the other hand, at the Si(111)–H interface such a charged layer is in principle absent. Removal of the electric field, and consequently the EFISH contribution, can be responsible for the decrease in the SHG intensity and the change in the phase of the ∂_{33} component. A number of studies have shown the sensitivity of SHG to the oxide charge.[20,30–34] Mitchell *et al.* excluded EFISH being responsible for the difference in the SHG–RA of Si(111)–H and Si(111)–SiO_2, because the samples used were relatively low-doped (n-type, 2 Ω cm resistivity) and the SHG response was found to be independent of dopant type and concentration.[25] We investigated the possibility of an EFISH contribution to SHG–RA at 800 nm: doping dependence and photomodulation studies show weak EFISH contribution at the Si(111)–SiO_2 interface.[35] On the basis of these studies, we concluded that EFISH is not responsible for the difference in the SHG–RA pattern of Si(111)–H and Si(111)–SiO_2 at 800 nm.

Downloaded 06 Sep 2009 to 129.32.36.173. Redistribution subject to AIP license or copyright; see http://jap.aip.org/jap/copyright.jsp

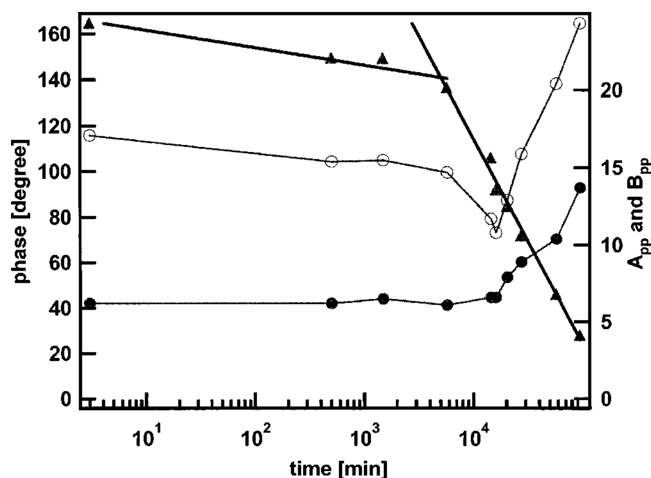

FIG. 2. The time evolution of the magnitude of isotropic, A_{pp} (●) and anisotropic, B_{pp} (○) components the A_{pp} and B_{pp} s as well as their relative phase (Δ_{AB}) (▲) as function of exposure to laboratory ambient (RH $=20\%-30\%$). Lines are guides for the eye. The SHG–RA data were collected on average every 3 days.

B. Oxidation of Si(111)–H followed by second-harmonic generation

The oxidation of the H terminated Si(111) surface can be followed by monitoring the SHG–RA patterns as a function of time of exposure to ambient. Under ambient laboratory conditions, 22 °C and 20% relative humidity (RH), a decrease of the magnitude of the SHG signal due to oxidation was observed first [Figs. 1(a)–1(b)]. It was followed by a phase change that was manifested by the reversal of the big peak/small peak sequence into the small peak/big peak sequence [Figs. 1(b)–1(c)]. Then an overall increase in SHG signal was observed and the SHG–RA pattern converged to that of the SiO_2/Si(111) [Figs. 1(c)–1(e)]. However, even after 40 days the SHG–RA pattern did not recover to that of SiO_2/Si(111). The SHG signal at $\phi=0°$ was about the half of that of the native oxide covered and the phase was 30° as opposed to 12° for the native oxide covered sample.

The evolution of the isotropic (A_{pp}), anisotropic (B_{pp}) components and their relative phase (Δ_{AB}) as function of time after hydrogen passivation are depicted in Fig. 2. Initially, Δ_{AB} decreases slowly from 160° to 140°. After about 3.5 days (~5000 min) Δ_{AB} begins to decrease rapidly, in a logarithmic fashion. A_{pp} and B_{pp} change non-monotonically as a function of time; an initial linear decrease, followed by a logarithmic increase in A_{pp} and B_{pp}.

We found in the evolution of phase Δ_{AB} both the slow and fast oxidation regimes previously reported by XPS studies.[7,8] We concluded that the SHG signal is sensitive to both the initial phase of oxidation—insertion of oxygen in Si backbonds—and the growth of multiple oxide layers. The SHG response is expected to be different when O is inserted in the Si backbonds. Even though the surface Si–H remains, the O inserted in the backbond will change the polarization of the Si–H bond. The length of the slow oxidation is shorter, 3.5 days, than the 5–7 day "induction" period assigned to insertion of ~0.7 ML oxygen in Si(100)–H.[7,8] The initial oxidation rate was calculated to be 2×10^{-6} ML/s by assuming that by the end of the induction period a 0.7 ML oxygen covers the Si(111) surface.

Once the bonds are established further change in the SH signal can be expected due to change is the electronic properties of the surface.[36] Angermann *et al.* found that the surface electronic properties, i.e., band bending and surface state density in the band gap follows the slow-fast-slow time evolution during oxidation of Si(111)–H.[36] During the logarithmic oxide growth region the decrease in the band bending was observed and correlated with the increase in the extrinsic states.[36] In the subsequent slow oxidation regime the change in band bending slowed down, accompanied by a decrease in the surface state density.[36] The similarity of the time evolution observed for the SHG phase (Fig. 2) and reported for the electronic properties at the interface, i.e., band bending and surface state density, leads us to conclude that SHG is sensitive to the changes of the electronic properties at the interface.

Graf *et al.* reported that the oxide thickness grew to 8–9 Å after half a year (measured by XPS), less than their reported thickness of ≈15 Å for native oxide.[7] The SHG–RA data indicate that the oxide and the Si–SiO_x interface formed by ambient oxidation are different from that of the native oxide (Fig. 1). The structural and chemical differences between the ambient formed and polished wafer oxides can come from the structure of the near Si–SiO_2 interface (thickness of transient SiO_x layer, distribution of oxidation states of Si in this layer), the density of defects in the oxide, and the density of oxide charges. These differences can then affect the SHG response of these different systems.

To better understand the change in the SHG signal, we carried out ellipsometric measurements in parallel with the SHG–RA experiments (Fig. 3). We observed a logarithmic growth of the ellipsometric oxide thickness that is preceded by a slow oxidation regime. The rate of the logarithmic oxide growth, determined from the ellipsometry measurement to be 0.74 nm/decade, is in good agreement with previous measurement (0.68 nm/decade).[37] It is evident that Δ_{AB} correlates with the ellipsometric thickness, [Fig. 3(b)]. The correlation of oxide thickness with A_{pp} and B_{pp} is more complicated. A_{pp} does not change until 0.9 nm oxide thickness, then increases with oxide thickness (not shown). B_{pp} first decreases with oxide thickness, then above 0.9 nm oxide thickness it increases with oxide thickness (not shown). Clearly, while Δ_{AB} does appear to correlate with the ellipsometric thickness, no simple correlation of A_{pp} or B_{pp} with the ellipsometry is apparent.

Discrepancies in the ellipsometry measurements reported here and in the literature should be pointed out. The formation of monolayer of a SiO_2 on Si(100), equivalent to a 3-Å-thick oxide layer is reported to require 15–20 days of storage in air.[7] Even after half a year oxide thickness 8–9 Å is reported.[7] However, we observe ~1 nm oxide thickness after 2 weeks of air exposure (Fig. 3). The discrepancy can arise from an over estimate of the oxide thickness by ellipsometry.[38] Acetone or benzene rinses can decrease the ellipsometric thickness, attributed to the removal of a "grease" film grown on the oxide with total thickness 3–4 Å after 24 h air exposure.[39] Graf *et al.* determined the oxide

Downloaded 06 Sep 2009 to 129.32.36.173. Redistribution subject to AIP license or copyright; see http://jap.aip.org/jap/copyright.jsp

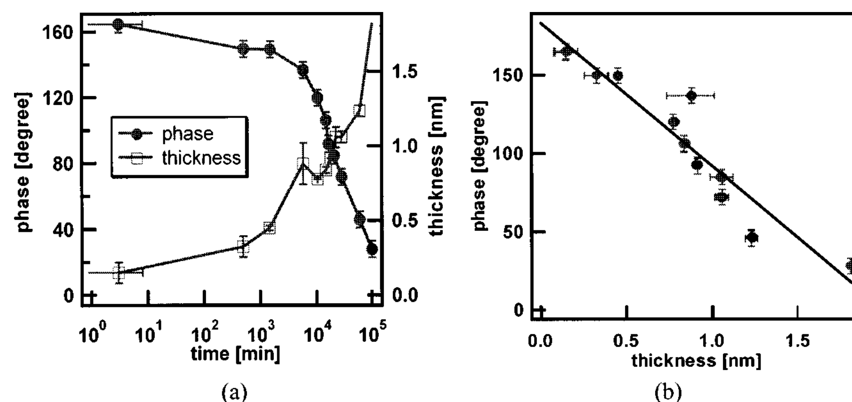

FIG. 3. (a) Oxide thickness determined by ellipsometry is indicated by open squares. Phase from rotational anisotropy is indicated by filled circles. (b) Correlation between ellipsometric oxide thickness and rotational anisotropy phase. The SHG–RA data were collected on average every 3 days.

thickness using XPS by taking the ratio of Si 2*p* peaks (Si^0 elemental and Si^{4+}O bound).[7] Perhaps we measure thicker oxides because of contamination from the air (e.g., organics that stick to the surface, which is not cleaned during storage in air). Other differences can arise from the storage conditions of the samples. Graf *et al.* stored the Si(100), *p*-type, 3–6 Ω cm wafers in single wafer packages made of polycarbonate and welded in transparent polyethylene bags. The relative humidity was 35%–40% during packaging.[7] We kept the samples exposed to the laboratory air (20% RH, temperature 23 °C). Our samples were also subjected to brief occasional laser irradiation, required for SHG measurements, which can accelerate the oxidation. Clearly, further study is required to resolve this issue.

The 2 Å oxide thickness on the freshly prepared Si(111)–H measured by ellipsometry is somewhat surprising (Fig. 3). An oxide thickness of 0 Å is expected, because the NH_4F treatment of clean Si(111)–SiO_2 results in complete oxide removal and H termination. Nonzero oxide thickness on HF treated Si was reported previously.[40,41] In contrast, Cicero *et al.* reported 0 Å oxide thickness for Si(111)–H.[42] The ellipsometric oxide thickness here was obtained assuming that the Si–SiO_2 interface only consists of two media. However, not only the overlayer oxide film but also the surface roughness affects the ellipsometric data.[43–45] Therefore, the film thickness plotted in Fig. 3 should be considered as the effective thickness but not necessarily the real one. As the oxide thickness increases, the real Si–SiO_2 system approaches to the two-layer model. We suggest that the 2Å "residual film" measured by ellipsometry is due to the roughness of the surface. The presence of a thin transition layer, associated with Si–H, of optical properties intermediate between bulk Si and air could also explain the nonzero oxide thickness found initially.

The mechanism of oxidation of Si–H is much debated. It is known that pure O_2, N_2, and H_2O do not react with Si–H surface below 300 °C.[46,47] Thus, it is puzzling that the oxidation of Si–H in ambient is widely reported. We would like to point out that in this study we did not attempt to control the ambient other than the relative humidity and temperature and did not investigate the mechanism of the oxidation process. Further studies in a controlled environment may point to the active species that are responsible for the oxidation in ambient. The results of this article demonstrate that SHG–RA would be ideally suited in these studies to follow the transformation of the surface to further elucidate the mechanism of oxidation of H–Si.

IV. CONCLUSIONS

SHG–RA provides a convenient means to monitor the chemical state of the Si surfaces, and to follow the conversion of H terminated surface to SiO_2 by oxidation as a function of time in ambient. The change in SHG–RA, in particular the relative phase, was shown to correlate well with the ellipsometric thickness. SHG is sensitive to the initial stage of oxidation (induction period) as well as to the logarithmic oxide growth. SHG is sensitive to the electronic properties of the surface, therefore it is a good probe of the quality of H terminated Si(111) surface. Under ambient conditions, the initial oxidation rate is at most 2×10^{-6} ML/s.

[1] D. J. Doren, Adv. Chem. Phys. **95**, 1 (1996).
[2] H. Waltenburg and J. T. Yates, Surface Chemistry of Silicon **95**, 1589 (1994).
[3] G. S. Higashi, Y. J. Chabal, G. W. Trucks, and K. Raghavachari, Appl. Phys. Lett. **56**, 656 (1990).
[4] R. A. Wolkow, Annu. Rev. Phys. Chem. **50**, 413 (1999).
[5] M. Niwano, J. Kageyama, K. Kurita, K. Kinashi, I. Takahashi, and N. Miyamoto, J. Appl. Phys. **76**, 2157 (1994).
[6] M. Morita, T. Ohmi, E. Hasegwa, M. Kawakami, and K. Suma, Appl. Phys. Lett. **55**, 562 (1989).
[7] D. Gräf, M. Grundner, R. Schulz, and L. Mühlhoff, J. Appl. Phys. **68**, 5155 (1990).
[8] M. R. Houston and R. Maboudian, J. Appl. Phys. **78**, 3801 (1995).
[9] G. J. Kluth and R. Maboudian, J. Appl. Phys. **80**, 5408 (1996).
[10] D. Gräf, M. Grundner, and R. Schulz, J. Vac. Sci. Technol. A **7**, 808 (1989).
[11] G. Mende, J. Finister, D. Flamm, and D. Schulze, Surf. Sci. **128**, 169 (1983).
[12] P. A. M. vanderHeide, M. J. BaanHofman, and J. J. Ronde, J. Vac. Sci. Technol. A **7**, 1719 (1989).
[13] A. Licciardello, D. Puglisi, and S. Pignataro, Appl. Phys. Lett. **48**, 41 (1986).
[14] H. Luo, C. E. D. Chidsey, and Y. Chabal, Mater. Res. Soc. Symp. Proc. **477**, 415 (1997).
[15] P. Dumas and Y. J. Chabal, Chem. Phys. Lett. **181**, 537 (1991).
[16] *Handbook of Optical Constants of Solids*, edited by E. D. Palik, (Academic, San Diego, 1998).

Downloaded 06 Sep 2009 to 129.32.36.173. Redistribution subject to AIP license or copyright; see http://jap.aip.org/jap/copyright.jsp

[17] G. Lüpke, D. J. Bottomley, and H. M. van Driel, J. Opt. Soc. Am. B **11**, 33 (1994).
[18] D. Bodlaki and E. Borguet, Rev. Sci. Instrum. **71**, 4050 (2000).
[19] H. M. van Driel, Phys. Rev. B **35**, 8166 (1987).
[20] V. Fomenko, J. F. Lami, and E. Borguet, Phys. Rev. B **63**, 121316 (2001).
[21] D. Bodlaki and E. Borguet (unpublished).
[22] J. A. Litwin, J. E. Sipe, and H. M. Van Driel, Phys. Rev. B **31**, 5543 (1985).
[23] J. E. Sipe, D. L. Moss, and H. M. van Driel, Phys. Rev. B **35**, 1129 (1987).
[24] V. Fomenko, D. Bodlaki, C. Faler, and E. Borguet, J. Chem. Phys. **116**, 6745 (2002).
[25] S. A. Mitchell, R. Boukherroub, and S. Anderson, J. Phys. Chem. B **104**, 7668 (2000).
[26] W. Monch, in *Semiconductor Surfaces and Interfaces*, Springer Series in Surface Science, Vol. 26, edited by G. Ertl *et al.* (Springer, Berlin, 2001).
[27] *CRC Handbook of Chemistry and Physics*, edited by D. R. Lide (CRC Press, Boca Raton, FL, 1997).
[28] D. Bodlaki, E. Freysz, and E. Borguet, J. Chem. Phys. **119**, 3958 (2003).
[29] *The* $Si-SiO_2$ *System*, edited by P. Balk, (Elsevier, Amsterdam, 1988).
[30] V. Fomenko, C. Hurth, T. Ye, and E. Borguet, J. Appl. Phys. **91**, 4394 (2002).
[31] J. Bloch, J. G. Mihaychuk, and H. M. van Driel, Phys. Rev. Lett. **77**, 920 (1996).
[32] J. G. Mihaychuk, J. Bloch, Y. Liu, and H. M. van Driel, Opt. Lett. **20**, 2063 (1995).
[33] J. G. Mihaychuk, N. Shamir, and H. M. van Driel, Phys. Rev. B **59**, 2164 (1999).
[34] N. Shamir, J. G. Mihaychuk, H. M. van Driel, and H. J. Kreuzer, Phys. Rev. Lett. **82**, 359 (1999).
[35] J. Fiore, V. Fomenko, D. Bodlaki, and E. Borguet (unpublished).
[36] H. Angermann, W. Henrion, and A. Roseler, in *Silicon-Based Materials and Devices*, edited by H. S. Nalwa (Academic, New York, 2001), pp. 268–298.
[37] F. Lukes, Surf. Sci. **30**, 91 (1971).
[38] S. I. Raider, R. Flitsch, and M. J. Palmer, J. Electrochem. Soc. **122**, 413 (1975).
[39] R. J. Archer, J. Electrochem. Soc. **104**, 619 (1957).
[40] K. Utani, T. Suzuki, and S. Adachi, J. Appl. Phys. **73**, 3467 (1993).
[41] G. Gould and E. A. Irene, J. Electrochem. Soc. **135**, 1535 (1988).
[42] R. L. Cicero, M. R. Linford, and C. E. D. Chidsey, Langmuir **16**, 5688 (2000).
[43] D. E. Aspnes, J. Vac. Sci. Technol. **17**, 1057 (1980).
[44] D. E. Aspnes, Phys. Rev. B **41**, 10334 (1990).
[45] E. D. Palik, V. M. Bermudez, and O. J. Glembocki, J. Electrochem. Soc. **132**, 871 (1985).
[46] X. Zhang, E. Garfunkel, Y. J. Chabal, S. B. Christman, and E. E. Chaban, Appl. Phys. Lett. **79**, 4051 (2001).
[47] X. Zhang, Y. J. Chabal, S. B. Christman, E. E. Chaban, and E. Garfunkel, J. Vac. Sci. Technol. A **19**, 1725 (2001).

Downloaded 06 Sep 2009 to 129.32.36.173. Redistribution subject to AIP license or copyright; see http://jap.aip.org/jap/copyright.jsp